Charge-Transport Properties of the 1,4-Diiodobenzene Crystal: A Quantum-Mechanical Study

Roel S. Sánchez-Carrera, Veaceslav Coropceanu,* Eung-Gun Kim, and Jean-Luc Brédas*

School of Chemistry and Biochemistry and Center for Organic Photonics and Electronics, Georgia Institute of Technology, Atlanta, Georgia 30332-0400

Received April 22, 2008. Revised Manuscript Received June 25, 2008

The 1,4-diiodobenzene (DIB) crystal stands out among molecular organic semiconducting crystals because of its remarkable room-temperature hole mobility (>10 $cm^2/(V\ s)$). Here, on the basis of a density functional theory study, we demonstrate that the high mobility in DIB is primarily associated with the heavy iodine atoms. We find that along specific crystal directions, both electrons and holes are characterized by a very small effective mass of about 0.5 m_0. Interestingly, iodine substitution also leads to a significant decrease in the local hole-vibration coupling compared to benzene; as a result, the electronic coupling for holes is calculated to be much larger than the hole-vibration coupling, which is consistent with the observation of large hole mobility. In marked contrast, the polaron binding energy in the case of electrons is found to be significantly higher than the electronic coupling; this implies that electrons in DIB are strongly localized even at room temperature.

Introduction

Oligoacenes, the polycyclic aromatic hydrocarbons composed of linearly fused benzene rings, and their derivatives represent the most studied and promising class of π-conjugated organic semiconductors used as active elements in new generations of (opto)electronic devices.[1−5] Recent efforts to improve the synthetic routes and the purification level have led to room-temperature charge-carrier mobilities that exceed 1 $cm^2/(V\ s)$.[5−12] Many attempts have been made to enhance the charge-transport properties of the parent acenes via substitution or functionalization.[2,3,5,13,14] Following this strategy, several halogen-substituted systems[15−18] have been prepared and investigated. For instance, the chlorosubstitution of tetracene to obtain 5,11-dichlorotetracene transforms the characteristic herringbone packing motif of tetracene into a slipped π-stacking motif[18] and leads to a slightly larger field-effect mobility (1.6 vs 1.3 $cm^2/(V\ s)$). It was also found that perfluorination can convert pentacene from a p-channel to an n-channel semiconductor.[15,16]

Interestingly, the largest impact of halogenation on charge-transport properties has been reported more than four decades ago for 1,4-diiodobenzene (DIB, see Figure 1),[19] a derivative of benzene (the building unit of the acenes). Photoconductivity measurements[19] revealed that DIB exhibits a room-temperature hole mobility as large as 12 $cm^2/(V\ s)$. In spite of this promising finding,[19] charge transport in DIB was revisited only very recently by Ellman et al.[20,21] These authors confirmed the earlier data regarding large hole mobility. In addition, the analysis of the electronic density of states derived from band-structure calculations[20] underlined the role played by the iodine atoms in the charge transport. It is also useful to note that DIB was investigated as a candidate to undergo a pressure-induced insulator-to-metal transition[22] and that its lattice dynamics was thoroughly studied both experimentally[23] and theoretically.[24]

* Corresponding authors. E-mail: coropceanu@gatech.edu (V.C.); jean-luc.bredas@chemistry.gatech.edu (J.-L.B.).

(1) Bredas, J. L.; Beljonne, D.; Coropceanu, V.; Cornil, J. *Chem. Rev.* **2004**, *104*, 4971–5003.
(2) Bendikov, M.; Wudl, F.; Perepichka, D. F. *Chem. Rev.* **2004**, *104*, 4891–4945.
(3) Anthony, J. E. *Chem. Rev.* **2006**, *106*, 5028–5048.
(4) Coropceanu, V.; Cornil, J.; da Silva Fihlo, D. A.; Olivier, Y.; Silbey, R.; Bredas, J. L. *Chem. Rev.* **2007**, *107*, 2165–2165.
(5) Anthony, J. E. *Angew. Chem., Int. Ed.* **2008**, *47*, 452–483.
(6) Podzorov, V.; Menard, E.; Borissov, A.; Kiryukhin, V.; Rogers, J. A.; Gershenson, M. E. *Phys. Rev. Lett.* **2004**, *93*, 086602.
(7) Podzorov, V.; Pudalov, V. M.; Gershenson, M. E. *Appl. Phys. Lett.* **2003**, *82*, 1739–1741.
(8) Podzorov, V.; Sysoev, S. E.; Loginova, E.; Pudalov, V. M.; Gershenson, M. E. *Appl. Phys. Lett.* **2003**, *83*, 3504–3506.
(9) Jurchescu, O. D.; Baas, J.; Palstra, T. T. M. *Appl. Phys. Lett.* **2004**, *84*, 3061–3063.
(10) Karl, N. *Synth. Met.* **2003**, *133*, 649–657.
(11) Karl, N.; Kraft, K. H.; Marktanner, J.; Munch, M.; Schatz, F.; Stehle, R.; Uhde, H. M. *J. Vac. Sci. Technol., A* **1999**, *17*, 2318–2328.
(12) Karl, N.; Stehle, R.; Warta, W. *Mol. Cryst. Liq. Cryst.* **1985**, *120*, 247–250.
(13) Coropceanu, V.; Kwon, O.; Wex, B.; Kaafarani, B. R.; Gruhn, N. E.; Durivage, J. C.; Neckers, D. C.; Bredas, J. L. *Chem.—Eur. J.* **2006**, *12*, 2073–2080.
(14) Kwon, O.; Coropceanu, V.; Gruhn, N. E.; Durivage, J. C.; Laquindanum, J. G.; Katz, H. E.; Cornil, J.; Bredas, J. L. *J. Chem. Phys.* **2004**, *120*, 8186–8194.
(15) Sakamoto, Y.; Suzuki, T.; Kobayashi, M.; Gao, Y.; Fukai, Y.; Inoue, Y.; Sato, F.; Tokito, S. *J. Am. Chem. Soc.* **2004**, *126*, 8138–8140.
(16) Sakamoto, Y.; Suzuki, T.; Kobayashi, M.; Gao, Y.; Inoue, Y.; Tokito, S. *Mol. Cryst. Liq. Cryst.* **2006**, *444*, 225–232.
(17) Perepichka, D. F.; Bendikov, M.; Meng, H.; Wudl, F. *J. Am. Chem. Soc.* **2003**, *125*, 10190–10191.
(18) Moon, H.; Zeis, R.; Borkent, E. J.; Besnard, C.; Lovinger, A. J.; Siegrist, T.; Kloc, C.; Bao, Z. N. *J. Am. Chem. Soc.* **2004**, *126*, 15322–15323.
(19) Schwartz, L. M.; Hornig, J. F. *Mol. Cryst.* **1967**, *2*, 379.
(20) Ellman, B. *J. Chem. Phys.* **2006**, *125*, 074702.
(21) Ellman, B.; Nene, S.; Semyonov, A. N.; Twieg, R. J. *Adv. Mater.* **2006**, *18*, 2284–2288.
(22) Brillante, A.; Della Valle, R. G.; Farina, L.; Venuti, E.; Cavazzoni, C.; Emerson, A. P. J.; Syassen, K. *J. Am. Chem. Soc.* **2005**, *127*, 3038–3043.
(23) Cramer, S. P.; Hudson, B. *J. Chem. Phys.* **1976**, *64*, 1140–1145.

10.1021/cm801108c CCC: $40.75
Published on Web 08/20/2008

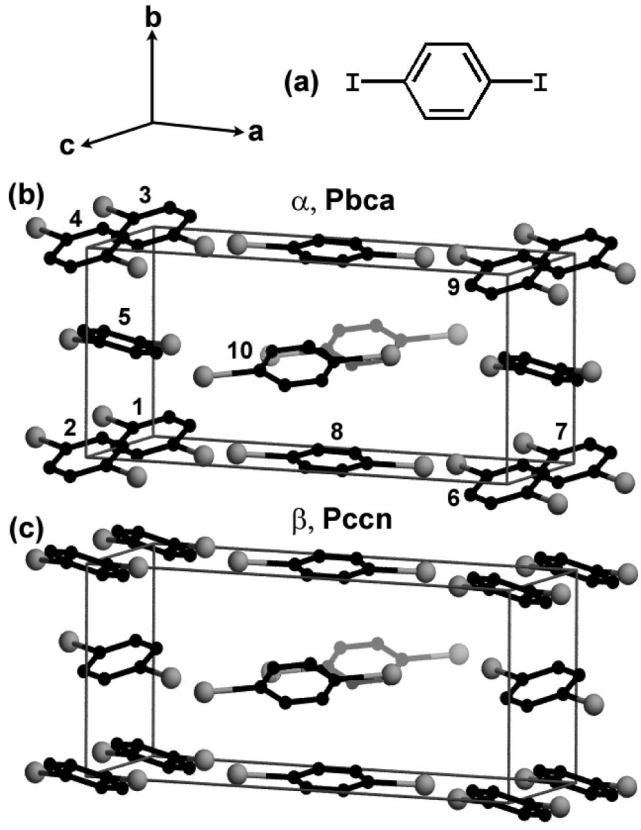

Figure 1. (a) Chemical structure of DIB. (b) Crystal structure of the α phase of DIB (*Pbca* space group, $a = 16.9697$, $b = 7.3242$, and $c = 6.156$ Å; the labeling of the DIB molecules as used in the calculations of the transfer integrals is also shown). (c) Crystal structure of the β phase of DIB (*Pccn* space group, $a = 17.047$, $b = 7.4370$, and $c = 6.1548$ Å).

Here, we report the results of a detailed quantum-mechanical study of the electronic and vibrational couplings in DIB; these are key parameters which determine the charge-transport properties in the crystal. We find that the iodine atoms have a strong effect on the transfer integrals and that there is a marked difference between the electron-vibration and hole-vibration couplings. Comparison with experiment and the parent benzene system will also be highlighted.

Methodology

The geometric and electronic structure of the isolated DIB and benzene molecules were obtained at the density functional theory (DFT) level by performing geometry optimizations with the B3LYP functional and the 6-31G(d,p) basis set for the carbon and hydrogen atoms and the 3-21G(d,p) basis set for the iodine atoms, as implemented in the Gaussian package.[25] Additional calculations, using the 6-311++G(d,p) diffuse functions for C and H atoms and the 6-311G basis set augmented[26] by two polarization (d and f) and two (s and p) diffuse functions for the iodine atoms, were also carried out in the case of the radical-anion states. The results of vibration calculations, performed at the B3LYP/6-31G(d,p) level of theory, were used to calculate the relaxation energy with the DUSHIN code.[27]

DIB forms two orthorhombic crystalline phases, denoted α and β, which belong to space group *Pbca* and *Pccn*, respectively,[28] and contain four molecules per unit cell (see Figure 1). The α phase (with lattice parameters[28] $a = 16.9697$ Å, $b = 7.3242$ Å, and $c = 6.156$ Å) is stable up to 326 K, where a transition to the β phase ($a = 17.047$ Å, $b = 7.4370$ Å, and $c = 6.1548$ Å) occurs. The geometry optimization of the crystal structures (with the lattice constants fixed at the experimental values), the derivation of the crystal electronic band structure, and the calculation of the optical vibrations at the Γ-point were performed using the CRYSTAL06 package.[29] In these calculations, the B3LYP functional and the 6-31G basis set (3-21G for the iodine atoms) and a uniform $4 \times 6 \times 8$ Monkhost-Pack *k*-point mesh were employed. Additional DFT/BLYP calculations using the Troullier-Martins pseudopotentials and plane wave basis sets with an energy cutoff of 70 Ry were also performed on the α-phase with the CPMD (Car−Parrinello Molecular Dynamics) code.[30] The inverse effective mass tensor was calculated by means of a numerical differentiation approach.[31]

Finally, the transfer integrals for nearest-neighbor pairs of molecules at the optimized crystal geometry were evaluated by using a fragment orbital approach[32] in combination with a basis set orthogonalization procedure.[33] These calculations were performed with the PW91 functional and Slater-type triple-ζ plus polarization (TZP) basis sets for all atoms, using the ADF (Amsterdam Density Functional) package.[34]

Results and Discussion

Molecular Electronic Structure. The frontier molecular orbitals (MOs) of DIB along with those of benzene are shown in Figure 2. As a result of iodine substitution, the D_{6h} symmetry of benzene is reduced to D_{2h} in DIB, which lifts the 2-fold orbital degeneracy of the frontier orbitals found in the parent benzene. Our calculations show that whereas the HOMO (highest occupied MO) level in the DIB molecule

(24) Della Valle, R. G.; Brillante, A.; Venuti, E.; Palazzi, L. *Chem. Phys. Lett.* **2000**, *325*, 599–604.
(25) Frisch, M. J.; Trucks, G. W.; Schlegel, H. B.; Scuseria, G. E.; Robb, M. A.; Cheeseman, J. R.; Montgomery, J. A., Jr.; Vreven, T.; Kudin, K. N.; Burant, J. C.; Millam, J. M.; Iyengar, S. S.; Tomasi, J.; Barone, V.; Mennucci, B.; Cossi, M.; Scalmani, G.; Rega, N.; Petersson, G. A.; Nakatsuji, H.; Hada, M.; Ehara, M.; Toyota, K.; Fukuda, R.; Hasegawa, J.; Ishida, M.; Nakajima, T.; Honda, Y.; KitaoO.; Nakai, H.; Klene, M.; Li, X.; Knox, J. E.; Hratchian, H. P.; Cross, J. B.; Bakken, V.; Adamo, C.; Jaramillo, J.; Gomperts, R.; Stratmann, R. E.; Yazyev, O.; Austin, A. J.; Cammi, R.; Pomelli, C.; Ochterski, J. W.; Ayala, P. Y.; Morokuma, K.; Voth, G. A.; Salvador, P.; Dannenberg, J. J.; Zakrzewski, V. G.; Dapprich, S.; Daniels, A. D.; Strain, M. C.; Farkas, O.; Malick, D. K.; Rabuck, A. D.; Raghavachari, K.; Foresman, J. B.; Ortiz, J. V.; Cui, Q.; Baboul, A. G.; Clifford, S.; Cioslowski, J.; Stefanov, B. B.; Liu, G.; Liashenko, A. Piskorz, P.; Komaromi, I.; Martin R. L.; Fox, D. J.; Keith, T.; Al-Laham, M. A.; Peng, C. Y.; Nanayakkara, A.; Challacombe, M.; Gill, P. M. W.; Johnson, B.; Chen, W.; Wong, M. W.; Gonzalez, C.; Pople, J. A. *Gaussian 03*, revision C.02; Gaussian, Inc.: Wallingford, CT, 2004.
(26) Glukhovtsev, M. N.; Pross, A.; Mcgrath, M. P.; Radom, L. *J. Chem. Phys.* **1995**, *103*, 1878–1885.
(27) Reimers, J. R. *J. Chem. Phys.* **2001**, *115*, 9103–9109.
(28) Alcobe, X.; Estop, E.; Aliev, A. E.; Harris, K. D. M.; Rodriguez-Carvajal, J.; Rius, J. *J. Solid State Chem.* **1994**, *110*, 20–27.
(29) Dovesi, R.; Saunders, V. R.; Roetti, C.; Orlando, R.; Zicovich-Wilson, C. M.; Pascale, F.; Civalleri, B.; Doll, K.; Harrison, N. M.; Bush, I. J.; D'arco, P.; Llunell, M. *CRYSTAL06*; University of Torino: Torino, Italy, 2006.
(30) *CPMD*, 3.9.2; IBM Corp and Max-Planck-Institut für Festkörperforschung: Stuttgart, 2005.
(31) Kim, E.-G.; Coropceanu, V.; Gruhn, N. E.; Sánchez-Carrera, R. S.; Snoeberger, R.; Matzger, A. J.; Bredas, J. L. *J. Am. Chem. Soc.* **2007**, *129*, 13072–13081.
(32) Senthilkumar, K.; Grozema, F. C.; Bickelhaupt, F. M.; Siebbeles, L. D. A. *J. Chem. Phys.* **2003**, *119*, 9809–9817.
(33) Valeev, E. F.; Coropceanu, V.; da Silva Fihlo, D. A.; Salman, S.; Bredas, J. L. *J. Am. Chem. Soc.* **2006**, *128*, 9882–9886.
(34) *ADF*, 2005.01; Scientific Computing and Modeling NV: Amsterdam, 2005.

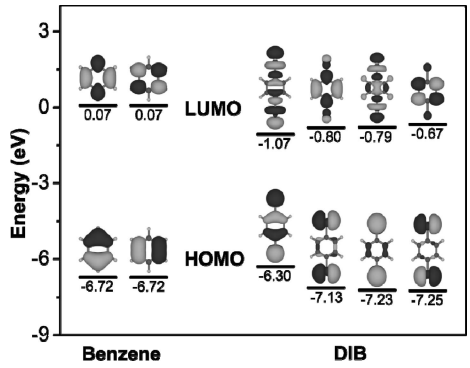

Figure 2. Illustration of the frontier molecular orbitals of benzene and DIB.

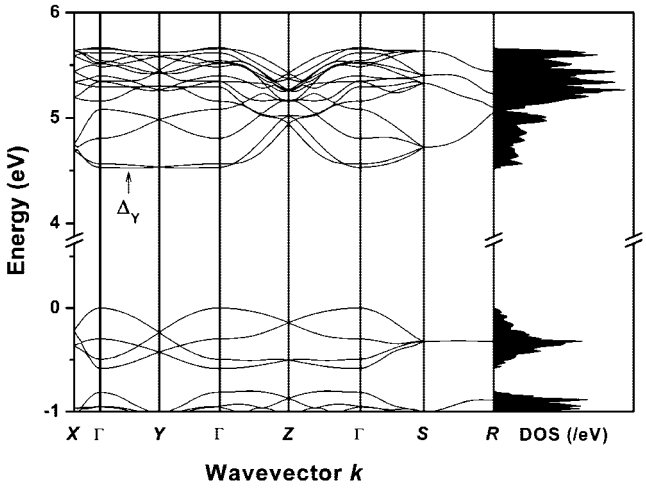

Figure 3. Electronic band structure of the α phase of DIB. Points of high symmetry in the first Brillouin zone are labeled as follows: Γ = (0,0,0), *X* = (0.5,0,0), *Y* = (0,0.5,0), *Z* = (0,0,0.5), *S* = (0.5,0.5,0), and *R* = (0.5,0.5,0.5), all in crystallographic coordinates. The zero of energy levels corresponds to the valence band edge. The conduction band edge denoted by Δ_Y = (0,0.25,0) is located about 4 meV below the Γ-point. The right panel illustrates the corresponding density of states.

is well separated (by about 0.8 eV) from the lower-lying MO levels, the energy difference between the LUMO (lowest unoccupied MO) and higher unoccupied MO levels is only about 0.3 eV. As seen from Figure 2, the wave functions of the frontier levels all display a significant electronic density on the iodine atoms; this suggests that the iodine atoms should contribute significantly to intermolecular electronic interactions for both electrons and holes. The HOMO−LUMO gap in DIB is reduced with respect to benzene by 1.4 eV, which is mainly due to the stabilization of the LUMO level.

Band Structure. The results of the band-structure calculations along various directions in the α and *β* crystalline phases of DIB are shown in Figures 3 and 4, respectively. In both cases, the valence band consists of four subbands arising primarily from the interactions among the HOMO levels of the four translationally inequivalent molecules present in the unit cell. This is confirmed by a comparison of Figures 2 and 5, which shows that the electron density of the four subbands at the Γ-point resembles that of the HOMO level. The upper valence subband has nearly the same structure in both crystalline phases. Its maximum is located at the Γ-point and the largest dispersion is observed along the *a*-axis (along Γ*X*) followed by a relatively weaker

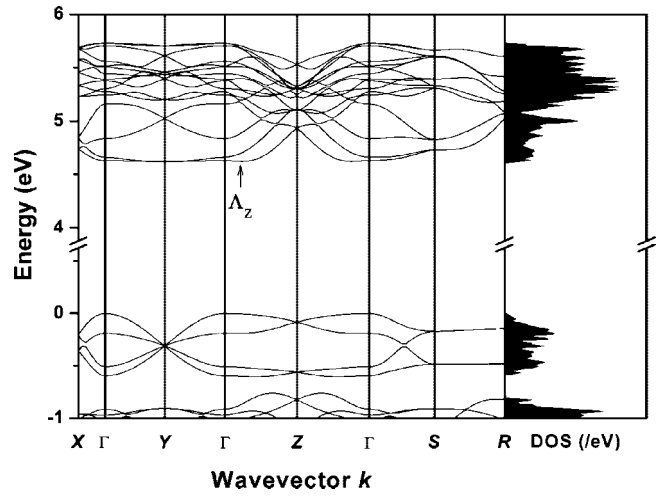

Figure 4. Electronic band structure of the *β* phase of DIB. The labeling scheme for the points of high symmetry is the same as in Figure 3. The conduction band edge denoted by Λ_Z = (0,0,0.125) is located about 7 meV below the Γ-point.

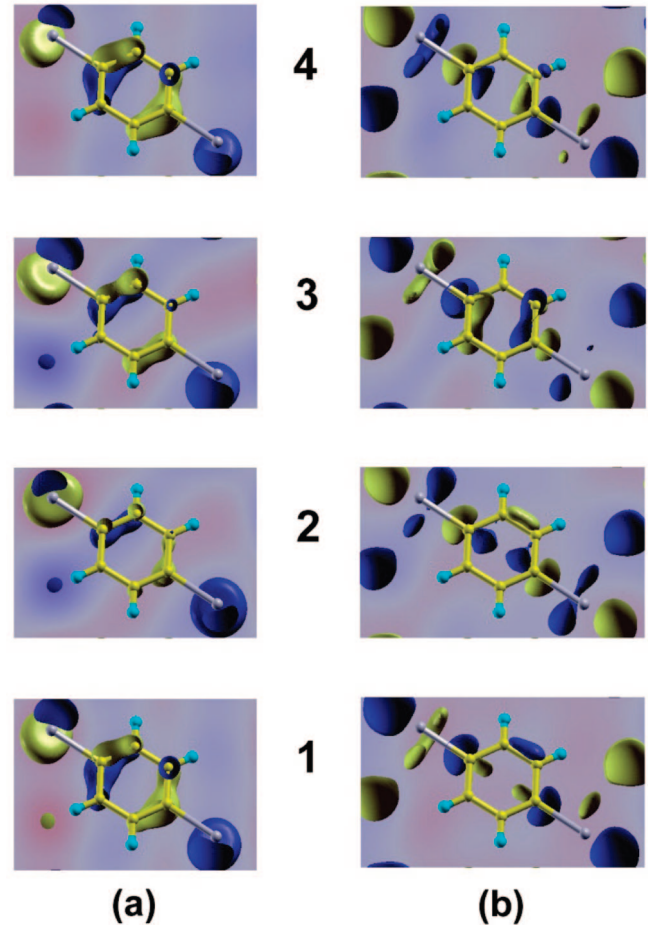

Figure 5. Wave functions of (a) the four valence subbands and (b) the four lowest conduction subbands at the Γ-point in the α crystalline phase (the frontier orbitals are denoted as 1). Because of the periodic boundary conditions, portions of the electron density appear as fragmented throughout the unit cell.

dispersion along the *b*-axis (Γ*Y*), whereas the dispersion along the *c*-axis (ΓZ), albeit smaller, remains significant.

Interestingly, the largest dispersion is observed along the direction where the intermolecular distance between adjacent molecules along the crystal axis is about 17 Å. Because such

Table 1. DFT Estimates of the Transfer Integral for Molecular Pairs in the α Phase of DIB

	hole (meV)	electron (meV)
$t_{1,2}$	−5	10
$t_{1,3}$	3	−5
$t_{1,7}$	0	0
$t_{1,5}$; $t_{4,5}$	−12	−20
$t_{2,10}$; $t_{9,10}$	46	9
$t_{1,8}$; $t_{6,8}$	−33	−104

a large intermolecular distance precludes any direct electronic coupling,[33] it is clear that the significant band dispersion seen along the *a*-axis is due to mediation of the electronic coupling by other molecules located in the *ab* and/or *ac* crystal planes. To shed more light on this issue, we computed the transfer integrals between all relevant neighboring molecules; the calculations were limited to the transfer integrals involving only the HOMO's for holes and the LUMO's for electrons. The results obtained for the α crystalline phase are collected in Table 1. As expected, the coupling between two consecutive molecules along the *a*-axis (molecules 1 and 7 in Figure 1) is zero. The transfer integrals along other two crystallographic directions are also very small. However, we found moderate coupling between adjacent molecules along the diagonal directions of both *ab* and *ac* planes, 46 and 33 meV, respectively. We note that if we were to replace DIB with benzene while keeping the same intermolecular distances, the transfer integrals would decrease by at least one order of magnitude; this confirms that the electronic coupling in DIB is largely dominated by iodine−iodine interactions.

As in the case of the valence band, the structure of the conduction band is very similar for both crystalline phases. The conduction band is in general more complex than the valence band. As discussed above, the LUMO level in DIB is separated from the next molecular levels by a very small energy gap; as a result, these upper-lying states are also expected to contribute to the conduction band. This is confirmed by the comparison of Figures 2 and 5, which indicates a significant contribution of the LUMO+2 state to the lower two conduction subbands. Furthermore, inspection of Figures 3 and 4 reveals that the conduction band consists of a larger number of subbands than the valence band. The conduction band minimum in both crystalline phases is shifted from the Γ-point and is located at $\Delta_Y = (0,0.25,0)$ and $\Lambda_Z = (0,0,0.125)$ for the α and β phases, respectively.

The dispersion of the lowest conduction subband is largest along the *a*-axis, where its bandwidth is comparable to that of the highest valence subband (165 vs 235 meV). At first glance, this would appear to contradict the results obtained for the transfer integrals in Table 1. Indeed, the largest transfer integrals coming from the LUMO interactions are at least twice as large as those derived for the HOMO's; one would then expect the conduction band to be significantly wider than the valence band. However, as was already mentioned, the conduction band arises from interactions among several molecular levels. Thus, the transfer integrals related to the LUMO's are not sufficient to rationalize the dispersion of the conduction band (this result again warns against a naive use of just HOMO's and LUMO's for the interpretation of charge-transport properties).

Table 2. Hole and Electron Effective Masses *m* (in units of the electron mass at rest, m_0) at the Band Edges of the α Phase of DIB

	m/m_0	parallel to
holes at Γ	0.56	*a*
	2.55	*b*
	8.07	*c*
electrons at Δ_Y	0.50	*a*
	6.06	*b*
	0.96	*c*

Table 3. Hole and Electron Effective Masses *m* (in units of the electron mass at rest, m_0) at the Band Edges of the β Phase of DIB

	m/m_0	parallel to
holes at Γ	0.58	*a*
	1.73	*b*
	13.83	*c*
electrons at Λ_Z	0.79	*a*
	4.57	*b*
	$>10^a$	*c*

[a] Because of the flatness of the band, we were unable to derive an accurate value of the effective mass along this direction.

In the case of wide bands where the thermally populated levels remain close to the band edges, the description of charge transport can be simplified by using the effective mass approximation. The tensor for the inverse effective mass (m_{ji}) is given by

$$m_{ji}^{-1} = \frac{1}{\hbar^2}\frac{\partial^2 \varepsilon}{\partial k_j \partial k_i} \quad (1)$$

Here, subscripts *i* and *j* denote the Cartesian coordinates in reciprocal space, ε the band energy, $\hbar$ the Planck constant and *k* the momentum. The calculated effective masses along the principal axes are shown in Table 2 and Table 3 for the α and β crystalline phases, respectively. As expected, the holes are found to be very light along the *a*-axis, with an effective mass of about 0.6 m_0 in both crystalline phases. The hole effective mass is about four times larger for the α phase and three times larger for the β phase along the *b*-axis, and is very large along the *c*-axis (8 m_0 and 14 m_0 for the α and β phases, respectively). For the sake of comparison, we note that the smallest effective mass for holes in the oligoacene family has been found in the case of rubrene (about 0.8 m_0).[35]

According to bandlike charge-transport theory, the carrier mobility in wide bands is given by

$$\mu = \frac{q\tau}{m} \quad (2)$$

where *q* is the carrier charge, τ the mean free time between collisions (or the mean relaxation time of the band state), and *m* the effective mass of the charge carrier. In the isotropic relaxation time approximation, the orientational anisotropy of the mobility is governed by that of the effective mass. In this context, it is interesting to note that the measured anisotropy of the hole mobility in DIB (the experimental hole mobilities at room temperature along the *a*-, *b*- and *c*-axes are reported to be 12, 4, and 1.7 $cm^2/(V\ s)$, respectively[19])

(35) Li, Z. Q.; Podzorov, V.; Sai, N.; Martin, M. C.; Gershenson, M. E.; Di Ventra, M.; Basov, D. N. *Phys. Rev. Lett.* **2007**, *99*, 016403.

Table 4. B3LYP/6-31G(d,p) (B3LYP/3-21G(d,p) for Iodine) Estimates of Intramolecular Frequencies (ω) and Polaron Binding Energy (Relaxation Energy) Related to Hole Transport in DIB

neutral		cation	
ω (cm^{-1})	E_{pol} (meV)	ω (cm^{-1})	E_{pol} (meV)
159	33.2	165	35.6
700	0.3	710	0.1
1074	23.9	1054	31.6
1217	8.4	1231	4.3
1614	21.8	1605	15.8
3226	0.1	3238	0.0
total	87.6	total	87.5

follows the same pattern as the calculated anisotropy of the hole effective mass.

The temperature dependence of mobility is determined (in the absence of chemical and physical defects) by the nature and strength of the electron−phonon (vibration) interactions. In the general case of the band model, mobility decreases as temperature increases. In the case of DIB, temperature-dependent measurements were performed only at elevated temperatures (above 200 K)[19,21] and the hole mobility was observed to decrease with increasing temperature. We note that, as such, this feature does not prove that charge transport in DIB is bandlike because at high temperatures a decrease in mobility with temperature could also take place in the hopping regime (in the so-called residual scattering limit where thermal energy exceeds the energy of the activation barrier[4]). However, this temperature dependence, taken together with the similarity between the orientational anisotropy of the mobility and the anisotropy of the effective mass, strongly points toward the bandlike nature of hole transport in DIB.

As in the case of holes, the smallest effective mass for electrons is obtained along the *a*-axis (0.5 m_0 and 0.8 m_0 for the α and β phases, respectively). Thus the effective mass for electrons in the α phase is even slightly smaller than that for holes. This result suggests that if the relaxation time of electrons were to be comparable to that of holes, their charge-transport properties should be also comparable, in particular along the *a*-axis. However, we will show in the next section that electron transport in DIB is expected to suffer from strong polaronic effects, which can explain that no charge transport has been reported for electrons.

Electron–Vibration Coupling. We now turn to a discussion of electron–vibration (phonon) interactions. In organic semiconductors, there are two major electron−phonon mechanisms: the first arises from the modulation of the site energy by vibrations and is referred to as local coupling, whereas the second mechanism arises from the modulation of the transfer integrals by intermolecular vibrations and is referred to as nonlocal coupling.[4]

The local electron−phonon coupling is the key interaction considered in Holstein's molecular crystal model[36,37] and in conventional electron transfer theory.[1,38] The overall strength of this coupling is expressed by the polaron binding (relaxation) energy E_{pol} or, in the context of electron transfer

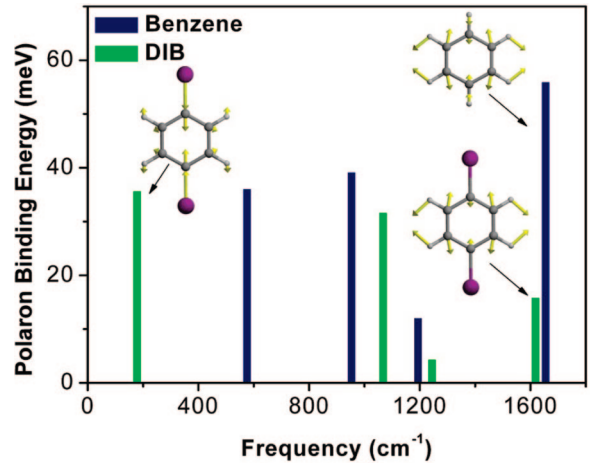

Figure 6. Contributions of the vibrational modes to the polaron binding energy (relaxation energy) in DIB and benzene.

theory, by the reorganization energy λ ($\approx 2E_{pol}$). It consists of both intra- and intermolecular contributions; the former reflects the changes in the geometry of individual molecules and the latter in the polarization of the surrounding molecules, upon going from the neutral to the charged state and vice versa. In the case of nonpolar molecules, the strength of the intermolecular contributions is expected to be much smaller than that of the intramolecular contributions.[4] Therefore, we focus here only on the intramolecular contributions to the local coupling.

The intramolecular reorganization energy can be computed either from adiabatic potential energy surfaces or from normal mode calculations.[1,13,39,40] The DFT estimates for hole–vibration coupling in DIB are collected in Table 4. For the sake of comparison, we also computed the hole–vibration coupling in benzene; the benzene and DIB results are illustrated in Figure 6. The intramolecular polaron binding energy calculated for DIB is about 88 meV, which is nearly 40% smaller than that in benzene (143 meV). The estimate for E_{pol} in benzene is in good agreement with the value of 122 meV derived by Kato and Yamabe in the framework of the one-electron approximation.[41] For the sake of comparison, we note that E_{pol} in pentacene is about 50 meV.[42,43]

As seen in Figure 6, the decrease in E_{pol} in DIB vs benzene results mostly from a significant drop in hole–vibration interaction for the high frequency mode at 1600 cm^{-1}; the coupling with all other modes is also reduced to some extent. The significant decrease in hole–vibration interaction with the 1600 cm^{-1} mode can be rationalized in terms of orbital vibronic coupling constants.[44,45] According to this model,

(36) Holstein, T. *Ann. Phys. (N. Y.)* **1959**, *8*, 325–342.
(37) Holstein, T. *Ann. Phys. (N. Y.)* **1959**, *8*, 343–389.
(38) Barbara, P. F.; Meyer, T. J.; Ratner, M. A. *J. Phys. Chem.* **1996**, *100*, 13148–13168.
(39) Malagoli, M.; Coropceanu, V.; da Silva Filho, D. A.; Bredas, J. L. *J. Chem. Phys.* **2004**, *120*, 7490–7496.
(40) da Silva Filho, D. A.; Coropceanu, V.; Fichou, D.; Gruhn, N. E.; Bill, T. G.; Gierschner, J.; Cornil, J.; Bredas, J. L. *Philos. Trans. R. Soc London, Ser. A* **2007**, *365*, 1435–1452.
(41) Kato, T.; Yamabe, T. *J. Chem. Phys.* **2001**, *115*, 8592–8602.
(42) Coropceanu, V.; Malagoli, M.; da Silva Filho, D. A.; Gruhn, N. E.; Bill, T. G.; Bredas, J. L. *Phys. Rev. Lett.* **2002**, *89*, 275503.
(43) Gruhn, N. E.; da Silva Filho, D. A.; Bill, T. G.; Malagoli, M.; Coropceanu, V.; Kahn, A.; Bredas, J. L. *J. Am. Chem. Soc.* **2002**, *124*, 7918–7919.
(44) Bersuker, I. B. *The Jahn-Teller Effect*; Cambridge University Press: Cambridge, U.K., 2006.
(45) Kato, T.; Yamabe, T. *J. Chem. Phys.* **2005**, *123*, 024301.

the hole–vibration coupling is large when the molecular deformation along the corresponding normal coordinate considerably distorts the electron density of the related MO (HOMO in the present case), leading to a large variation in the MO energy. The inspection of the normal coordinate for the 1600 cm^{-1} mode shows that the iodine atoms are not involved in this vibration (they stay motionless). Because part of the electron density in the case of the diiodobenzene HOMO is located on the iodine atoms, the energy of this molecular state is comparatively less affected by this vibration than for benzene; thus, the hole–vibrational coupling constant is smaller in the case of DIB.

The charge-transport properties of a particular system results from the interplay between a charge localization effect due to electron−phonon coupling and a charge delocalization effect due to the electronic coupling. The electronic coupling is defined by the transfer integrals or, alternatively, can be obtained from bandwidths. We recall that, in the case of complex systems, it is incorrect to take the bandwidth of the entire valence or conduction band as a measure of the delocalization energy; rather, only those subbands that are thermally populated and contribute to charge transport should be considered. For the understanding of hole transport in DIB only the upper valence subband is relevant; in the α crystalline phase (the results for the β phase are similar), the related bandwidths are 218, 235 and 141 meV for the *a*-, *b*-, and *c*-directions, respectively. All these values are significantly larger than the polaron binding energy (88 meV). Thus, we come to the conclusion that local coupling does not lead to the formation of molecular-type (localized) polarons in DIB. However, it is important to bear in mind that even if charge transport in DIB falls in a bandlike regime, the local hole–phonon coupling is large enough to result in substantial polaronic effects which can lead to a renormalization of the effective mass. A complete description of this issue can be obtained only in the framework of a microscopic approach that treats the whole Hamiltonian self-consistently; this challenging task is beyond the scope of the present contribution.

There is growing consensus in the literature[4,46−48] that both local and nonlocal couplings should be taken into account in order to obtain a coherent description of charge transport in organic molecular crystals. The issue of nonlocal coupling is in general less well studied and understood than that of local coupling. However, in the case of DIB, our preliminary results suggest that nonlocal interactions are weak. This is consistent with the fact that, because the iodine atoms are heavy, the amplitudes of DIB molecular motions are in general very small and the modulation of the transfer integrals due to intermolecular vibrations can be expected to be small as well. The only modes characterized by large displacements correspond to librations around the I−I axis. Because the electronic coupling in DIB is dominated by iodine−iodine interactions, these modes are also expected to have only a small impact on the transfer integrals.[21] An example of the dependence of the transfer integral on the coordinate of the libration mode at 110 cm^{-1} is shown in Figure 7. For a geometric distortion of the dimer along this mode corresponding to the mean-squared displacement ($Q = \pm 2$) at room temperature, the transfer integral varies just by 10%, which supports the above arguments. Thus, nonlocal coupling appears not to be strong enough to lead to radical changes in the nature of hole transport in DIB, even if this term is likely to affect the relaxation time and consequently the temperature dependence of the mobility.

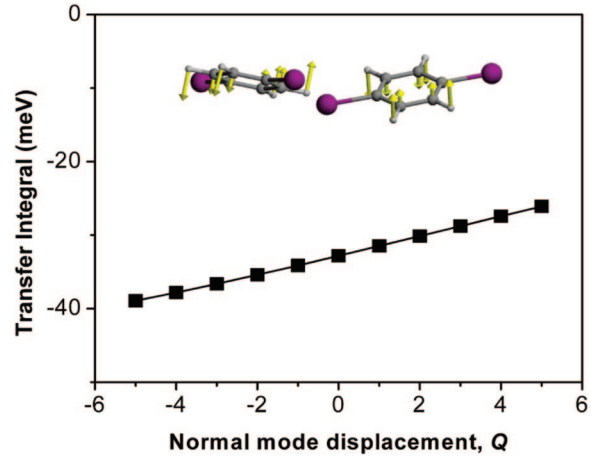

Figure 7. Evolution of the HOMO transfer integral for a DIB dimer composed of molecules 1 and 8, as a function of the dimensionless normal coordinate of the $\omega = 110$ cm^{-1} libration mode (here, the mean-square displacement at room temperature approximately corresponds to $Q = \pm 2$ because thermal energy at room temperature is ~200 cm^{-1}).

Although the iodine substitution of benzene results in a significant reduction in hole polaron binding energy, the situation is markedly different for electrons. It is well established that the electrochemical reduction of aromatic halides can cause the cleavage of the carbon−halogen bonds in the generated radical anions.[49,50] Electronic-structure calculations on monoiodobenzene have shown that the lowest potential surface exhibits a minimum along the C−I dissociation coordinate characterized by a very elongated C−I bond and with the negative charge localized on the halogen atom.[51] We have obtained similar results for the radical anion of DIB (see Figure 8). As seen from Figure 8, in contrast to the oxidized (radical cation) state where the symmetric geometry of the neutral state is preserved, the reduction of DIB results in extreme elongation (by about 0.8 Å) of one of the C−I bonds (a broken-symmetry effect). Such a large geometry deformation results in a very large polaron binding energy for electrons, 1.3 vs 0.088 eV for holes (in comparison, the polaron binding energy for electrons in benzene is about 0.2 eV).

The calculated electron polaron binding energy in DIB is much larger than the bandwidth of the lowest conduction subband. This result strongly suggests that in this case electron−phonon coupling leads to the formation of localized molecular polarons. In such an instance, charge transport can

(46) Della Valle, R. G.; Brillante, A.; Farina, L.; Venuti, E.; Masino, M.; Girlando, A. *Mol. Cryst. Liq. Cryst.* **2004**, *416*, 145–154.
(47) Hannewald, K.; Bobbert, P. A. *Appl. Phys. Lett.* **2004**, *85*, 1535–1537.
(48) Hannewald, K.; Stojanovic, V. M.; Schellekens, J. M. T.; Bobbert, P. A.; Kresse, G.; Hafner, J. *Phys. Rev. B* **2004**, *69*, 075211.
(49) Andrieux, C. P.; Blocman, C.; Dumasbouchiat, J. M.; Saveant, J. M. *J. Am. Chem. Soc.* **1979**, *101*, 3431–3441.
(50) Sanecki, P. *Comput. Chem.* **2001**, *25*, 521–539.
(51) Pierini, A. B.; Vera, D. M. A. *J. Org. Chem.* **2003**, *68*, 9191–9199.

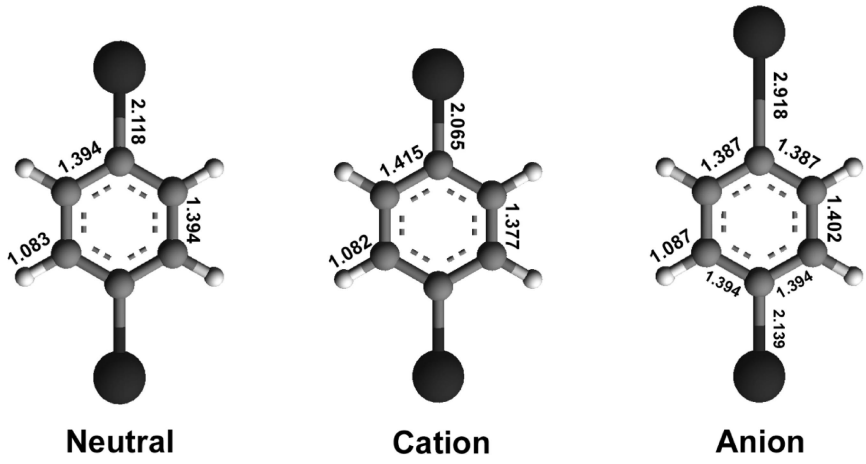

Figure 8. DFT geometries (bond lengths are given in Å) for the neutral, radical-cation, and radical-anion states of DIB.

be described as a sequence of uncorrelated hops. The corresponding activation energy is very large (half the polaron binding energy,[36,37] i.e., about 0.6 eV); according to the hopping model, the electron mobility in DIB should be vanishingly small even at room temperature. It would also be of interest to find out whether, upon electron injection, molecular fragmentation of DIB takes place in the solid state as well; such a fragmentation would obviously lead to the formation of chemical defects.

Conclusions

We have investigated the electronic and electron/hole–vibration interactions in the crystal of 1,4-diiodobenzene. The transfer integral and band-structure calculations confirm that the electronic coupling for both holes and electrons is dominated by iodine−iodine interactions. We have found that both types of charge carriers are characterized by a very small effective mass of about 0.5 m_0 (along the *a*-axis).

Our results indicate that the iodine substitution of benzene leads to a significant decrease in the local hole–vibration coupling and that the transfer integrals for holes are only moderately affected by intermolecular vibrations. The estimated values for bandwidth and polaron binding energy along with the results from effective mass calculations and temperature-dependent measurements all concur to suggest a bandlike transport regime for holes in DIB. However, low-temperature mobility measurements and additional theoretical investigations would be useful to reach a more complete description of hole transport in DIB.

In the case of electrons, the DFT calculations point to a very large polaron binding energy, which suggests that electrons are completely localized even at room temperature. The large relaxation energy (local electron–vibration coupling) calculated for the radical-anion of DIB is consistent with the previous findings that upon reduction, iodobenzenes[50] are prone to cleavage of the carbon−iodine bonds.

To summarize, our calculations on DIB indicate that iodine substitution could yield new organic semiconductors with large hole mobilities; however, these materials are likely to be less suitable as electron transport materials. Theoretical work on new iodine-substituted arylenes is currently under way. We hope that our results will trigger further experimental investigations on this interesting class of organic semiconductors.

Acknowledgment. We thank B. Ellman at Kent State University and J. F. Torres at the University of Torino for stimulating discussions. This work was partly supported by the Office of Naval Research and the National Science Foundation under the STC (DMR-0120967) and CRIF (CHE-0443564) programs.

CM801108C